Available online at www.sciencedirect.com
ScienceDirect
Journal of Crystal Growth 298 (2007) 625–630
JOURNAL OF CRYSTAL GROWTH
www.elsevier.com/locate/jcrysgro

MOVPE growth and real structure of vertical-aligned GaAs nanowires

J. Bauer[a,*], V. Gottschalch[a], H. Paetzelt[a], G. Wagner[b], B. Fuhrmann[c], H.S. Leipner[c]

[a]*Institut für Anorganische Chemie, Universität Leipzig, Johannesallee 29, D-04103 Leipzig, Germany*
[b]*Institut für Kristallographie und Mineralogie, Universität Leipzig, Linnestr. 5, D-04103 Leipzig, Germany*
[c]*Martin-Luther-Universität Halle, D-06099 Halle (Saale), Germany*

Available online 11 December 2006

Abstract

We studied the influence of the substrate preparation and the growth conditions important to fabricate GaAs nanowires (NWs) with metal-organic vapor phase epitaxy. The growth parameters temperature, precursor partial pressures and growth duration were investigated. The definite choice of the V/III ratio enables NW length growth independent on the diameter. By investigating the temporal evolution of the GaAs-NW growth a diameter-dependent growth rate could be determined. Applying nanosphere lithography arranged GaAs-NW arrays were achieved. The NWs morphology and real structure was investigated using (high-resolution) transmission electron microscopy and selective area diffraction. The twin formation in GaAs NWs was investigated. A crystallographic model is presented.

PACS: 61.46.+w; 68.65.−k; 78.67.−n; 81.15.Gh; 81.16.−c; 81.07.−b

Keywords: A1. Nanostructures; A3. Metal-organic vapor phase epitaxy; B2. Semiconducting gallium arsenide

1. Introduction

On the way of device miniaturization and efficiency intensification currently a special interest is pointed on semiconducting nanoscale structures. The III–V-semiconductor nanowires (NWs) promise an application in high-efficient optoelectronic building blocks.

Several techniques were investigated to obtain semiconductor NWs [1–3]. An important NW-growth model [4–6] bases on the vapor–liquid–solid (VLS) mechanism [7]. Hiruma et al. [8,9] examined previously the fabrication of free-standing GaAs NWs using metal-organic vapor phase epitaxy (MOVPE) with a special focus on structural and optical properties. Some typical MOVPE conditions were considered in more recently presented VLS-based growth models [10,11]. NW positioning in two-dimensional arranged arrays has been achieved using electron beam lithography [3] and nanoimprint lithography [12].

First, the substrate preparation with a thin gold film and the effect of annealing on the NW growth are discussed. Following, arranged GaAs-NW arrays are presented, which are achieved by the combination of nanosphere lithography and GaAs-NW growth. Then, we focus on basic studies concerning the VLS-growth process in MOVPE. Furthermore, structural properties are discussed. In particular, a geometrical model for the formation of rotational twins along the GaAs-NW axis is shown.

2. Experimental procedure

For NW growth the commercial MOVPE apparatus AIX200 is used in low-pressure mode (5 kPa) with a 7000 sccm total gas flow and H_2 atmosphere. As group-III precursor serves trimethylgallium (TMGa). Arsane (AsH_3) and tertiarybutyl-arsane (tBAs) are investigated as group-V source materials. Usually V/III ratios of 1 up to 100 are used. The GaAs NW growth occurs at temperatures $>400\,^{\circ}C$.

We use GaAs$(\bar{1}\,\bar{1}\,\bar{1})_{As}$ substrates to achieve a perpendicular NW growth [13]. In a thermal evaporator a gold film of a few nanometer thickness is deposited on the substrate. Using this preparation a dense and equable "lawn" of GaAs NWs is achieved (Fig. 1a). Otherwise, a 120 s annealing step at 600 °C leads to a particle formation with

*Corresponding author. Tel.: +49 34136206; fax: +49 34136249.
E-mail address: jbauer@uni-leipzig.de (J. Bauer).

0022-0248/$ - see front matter © 2006 Elsevier B.V. All rights reserved.
doi:10.1016/j.jcrysgro.2006.10.082

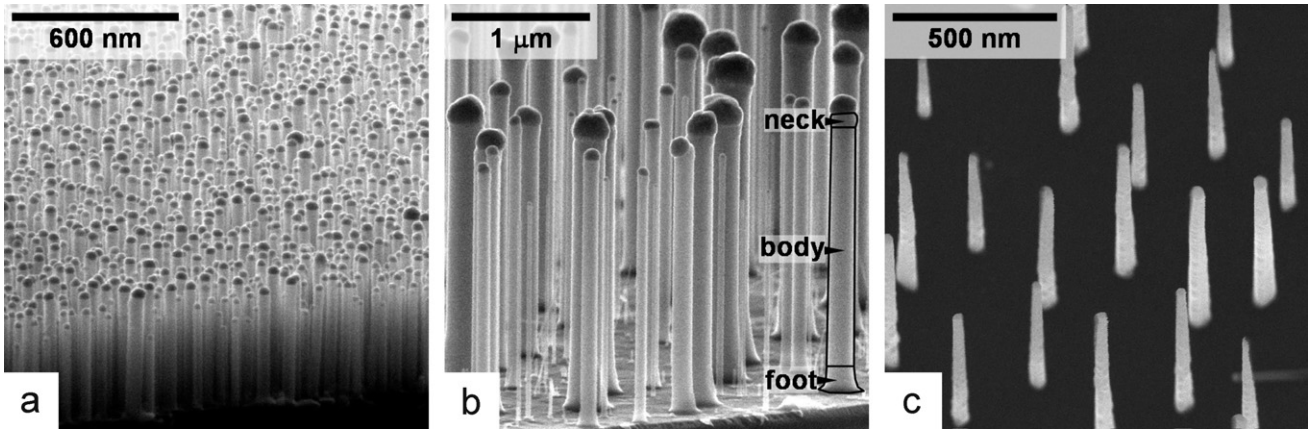

Fig. 1. Typical arrangement of GaAs NWs on GaAs $(\bar{1}\,\bar{1}\,\bar{1})_B$ substrate grown (a) without and (b) with an additional 600 °C temperature step after gold film evaporation to reach a broad diameter distribution. (c) The arranged gold cluster deposition using nanosphere lithography allows the fabrication of GaAs-nanowire arrays with honeycomb-like patterns.

a broad size distribution. This system forms the starting point for investigating the effect of the MOVPE-growth conditions on the NW growth with respect to the NWs' diameters (Fig. 1b). However, using gold evaporation the resulting GaAs NWs are randomly distributed over the substrate. To realize a regular NW arrangement, the GaAs substrates are covered with a monolayer of submicrometer sized polystyrene spheres. The spheres are provided from a liquid solution which is spinned on the substrate. Domains up to a few ten microns in size with perfectly, hexagonally arranged polystyrene spheres are formed. Between the spheres exist small triangular holes. After deposition of a thin gold layer using evaporation the polystyrene spheres are removed from the substrate. As a result, honeycomb-like patterns of gold triangles inside domains are left on the substrate. To avoid moving of the gold structures during temperature increase to growth temperature the gold arrays are fixed by a thin amorphous SiO_x layer deposited with plasma-enhanced chemical vapor deposition (PECVD). Fig. 1c illustrates the arranged GaAs-NW arrays fabricated with nanosphere lithography [14]. The diameters lie between 35–50 nm.

3. Results and discussion

3.1. MOVPE growth of GaAs NWs

In this section we will give a short overview of the extensive growth investigations, which will be reported in more detail elsewhere [15]. First, we focus on the effect of the V/III ratio on the GaAs-NW growth. To control the V/III ratio the group-V partial pressure is varied. For these experiments tBAs is used, because it allows a better adjustment of low partial pressures in our MOVPE system. We observed two situations. At low V/III ratios the growth rate of thicker NWs is increased compared to thinner ones (dotted curve in Fig. 2). In contrast, at high V/III ratios we find the opposite behavior (solid curve in Fig. 2). Several influences seem to be the reason for the change. The last

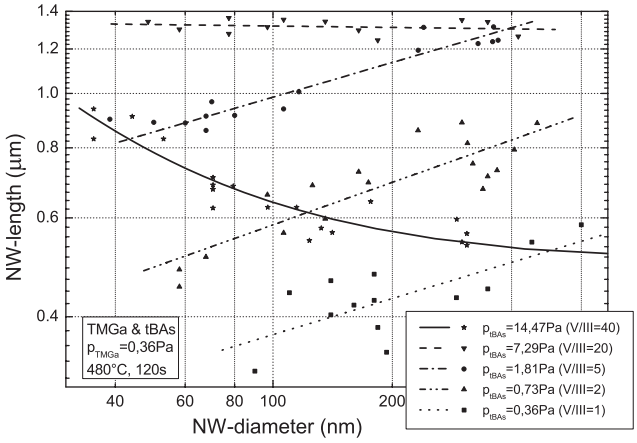

Fig. 2. NW length in dependence of the NW diameter for several V/III ratios by varying the tBAs partial pressure. At a medial partial pressure (V/III = 20) the growth becomes diameter independent.

case at high V/III ratios was previously observed and modeled by Seifert et al. [11]. Thus, the precursor pathway over the crystal surface is deciding for the NW growth in MOVPE. The case at low V/III ratios fits to the NW-growth model of Givargizov [4]. Here, the thermodynamic state of the droplet dominates the NW growth, which is influenced by the Gibbs–Thomson effect with respect to NW diameter. The growth rate limiting step of the VLS system is the crystallization at the droplet–crystal interface [4]. From the chemical point of view gallium and arsenic react in a solution with the solvent gold to form solid gallium arsenide. The reaction rate of this second order chemical reaction depends on the concentrations of the two reactants ($c_{Ga/As}$ for the gallium/arsenic concentration) in the liquid:

$$R_{GaAs} \propto c_{Ga} \cdot c_{As}. \quad (1)$$

Increasing the arsenic concentration in the liquid due to a higher tBAs gas-phase partial pressure, the equilibrium of the chemical reaction is driven toward GaAs formation. The gallium arsenide reaction rate R_{GaAs} increases. In the

experiment this behavior is observed by the increased growth rate of the two dash-dotted curves in Fig. 2. The diameter dependence is already given by the Gibbs–Thomson effect. However, the increase of both the arsenic concentration and the reaction rate leads to a drop of the gallium concentration in the droplet (Eq. (1)). If the arsenic concentration is too high, a lack of gallium appears in the droplet. Thus, the gallium supply determines the GaAs-NW growth (solid curve in Fig. 2). The experimental points are fitted by a $1/d$ dependence with the solid line [11]. The combination of both situations allows the growth of GaAs NWs independent of the diameter (dashed curve in Fig. 2).

Second, we discuss the temporal evolution of GaAs-NW growth. According to Fig. 2 we obtained the effect of growth duration (t_g) on the length (l) growth with respect to the diameter (d). To describe these curves more quantitatively, the data points are fitted by the empirical relation:

$$l = f \cdot d^e. \tag{2}$$

The parameters f and e reflect the dimension and the diameter dependence of length growth, respectively. Considering the Gibbs–Thomson effect, Givargizov [4] found the semi-empirical relation for the length growth rate: $R = \partial l/\partial t_g \propto \left(1/d_c - 1/d\right)^n$. The critical NW diameter d_c and the empirical exponent n appear. The comparison of both formulas with a view on the equality of the first derivatives, parameter e in Eq. (2) can be approximated: $e = nd_c/(d - d_c)$. If the diameters of the investigated NWs are much bigger than the critical diameter, parameter e changes only very slowly with the diameter and can be assumed as a constant. While in Givargizov's equation three parameters (proportionality factor, d_c, n) have to be fitted, Eq. (2) depends only on two independent parameters. The critical diameter can be estimated by: $d_c = 4\Omega\sigma/\Delta\mu$ [4]. The molar volume Ω, droplet surface tension σ and chemical potential difference $\Delta\mu$ depend on the droplet material. Because the real droplet composition during growth is not known, the two situations with a nearly pure gold droplet ($\Omega = 11.43\,\mathrm{cm^3/mol}, \sigma = 1.13\,\mathrm{J/m^2}$) and a gallium droplet ($\Omega = 10.21\,\mathrm{cm^3/mol}, \sigma = 0.71\,\mathrm{J/m^2}$) are distinguished. Assuming liquid phase epitaxy-like conditions for the GaAs crystallization ($\Delta\mu \approx 1\,\mathrm{kcal/mol}$) [16], the critical NW diameter is 11.0 and 7.3 nm for gold and gallium droplets, respectively. At common NW-growth conditions ($T_g = 480\,^\circ\mathrm{C}$, $p_{\mathrm{TMGa}} = 0.36\,\mathrm{Pa}$, $p_{\mathrm{AsH_3}} = 3.6\,\mathrm{Pa}$) we observed a lower limit for the NW thickness at about 10 nm, which matches well to the order of magnitude of the estimated values. The diameter range of 40–450 nm for the growth investigations is situated sufficiently far away from the critical diameter to justify the usage of Eq. (2). Both parameters are determined for growth durations in the range from 20–640 s for three V/III ratios. After an "initial growth", parameter e reaches a constant value for all three V/III ratios. Thus, after this "initial growth" period, the dependence of growth on the growth time is only given by parameter f. Parameter f shows a linear dependence on time: $f = f_0 \cdot t_g$ for all V/III ratios. Using Eq. (2) the growth rate can be expressed with respect to the diameter:

$$R = \frac{\partial l}{\partial t_g} = f_0 \cdot d^e. \tag{3}$$

The result is shown graphically in Fig. 3 for the three V/III ratios. The experiments are carried out with arsine as group-V source material. Thus, the results are not completely comparable with Fig. 2, but the strong effect of the V/III ratio on the diameter dependence of the growth rate is shown obviously.

3.2. Morphology

GaAs NWs consist of three different parts which are formed during the several stages of NW growth: a "foot", a "body" and a "neck" section [15]. On top of the NWs always the crystallized Au–Ga–As alloy droplet is observed. The NW-growth direction is $\langle \bar{1}\,\bar{1}\,\bar{1} \rangle_{\mathrm{As}}$.

The GaAs NWs grown within the temperature range of 400–530 °C are columnar-shaped with well-defined border planes. At higher temperatures the common vapor phase epitaxial layer growth processes lead to a lateral growth at the side facets of the NWs. Thus, a tapered morphology is observed.

The structure of the NWs was investigated using scanning electron microscopy (SEM), (high-resolution) transmission electron microscopy ((HR)TEM) and selective area diffraction (SAD), for which the samples were prepared by the "top-down" method. The GaAs NWs have sphalerite structure with a threefold rotational axis along the growth direction (Fig. 4). The NWs show extended $\{1\,1\,2\}$-border planes and narrow $\{1\,1\,0\}$-planes. With respect to the polarity the $\{1\,1\,2\}$-planes are different in size. In particular, the $\{1\,1\,2\}_{\mathrm{A}}$-planes are narrower than the $\{1\,1\,2\}_{\mathrm{B}}$-planes. Mareck et al. [17] investigated the wetting of In droplets on InP(1 1 1) substrates. Due to the

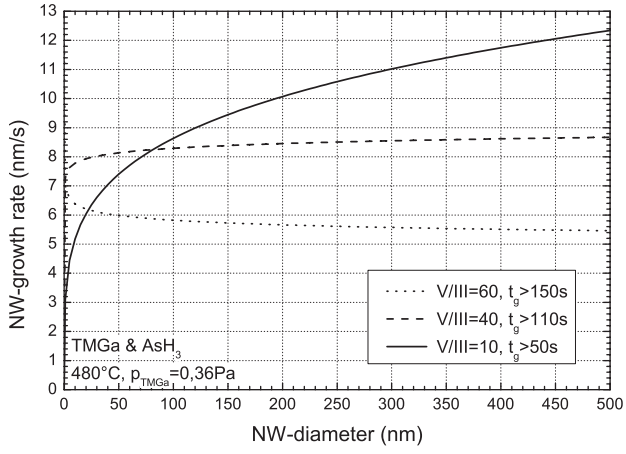

Fig. 3. Diameter-dependent growth rate for the growth of GaAs NWs at different V/III ratios. The model parameters f and e are determined for the diameter range from 40 to 450 nm. In the extrapolation to $d = 0$ nm the increasing diameter dependence of parameter e is neglected.

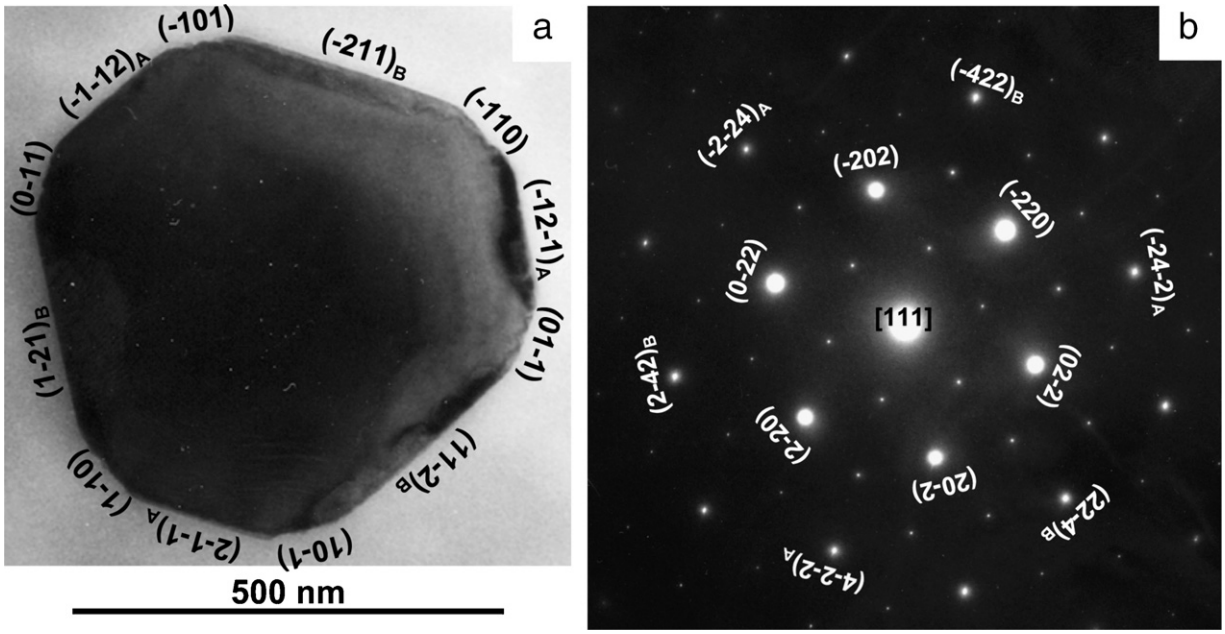

Fig. 4. The bright-field TEM image (a) shows the cross-section ((1 1 1)-plane) of a GaAs NW. Based on the SAD pattern (b) with beam direction parallel to [1 1 1] it is possible to identify the planes terminating the wire as shown in (a). The additional weak diffraction spots stem from parts with wurtzite-type structure due to stacking faults.

anisotropy of the surface tension of the substrate, the contact area of the droplets reflects the same threefold symmetry as the cross-section of the GaAs NWs. Possibly, the origin of the observed asymmetry is caused by the anisotropic wetting of the droplet.

3.3. Real structure

SEM investigations reveal notches at the surface of the GaAs NWs (Fig. 5a). The shape of the notches seems to have a definite geometry, which differs with the polarity of the border planes. The notches at the $\{1\,1\,2\}_A$-planes are more extended than at the $\{1\,1\,2\}_B$-planes. As shown on the bright-field TEM image, Fig. 5b, two-dimensional defects are stacked along the NW-axis. HRTEM imaging and SAD confirm the presence of twins (Fig. 5c,d). The planar boundaries between the twinned parts are coherent, i.e. they are dislocation-free. Where do these twins come from? Generally, a twin is formed by a 180° rotation of one crystalline part around the $\langle\bar{1}\,\bar{1}\,\bar{1}\rangle_{As}$-growth axis. Two ways are possible to explain the origin of such twins: (i) successive nucleation of partial dislocations at steps on the side planes and their slip on the (1 1 1) glide plane through the entire wire. Then the twin thickness is determined by the number of partials nucleated. In this way a groove at the starting point as well as at the opposite side will be formed [18]. Hence, the grooves are the result of plastic deformation. However, there is the question: Where does the driving force for dislocation nucleation come from? (ii) The twins are formed during the growth (so-called growth twins). Then, the initial step for twin nucleation is the incorporation of atoms at "wrong" lattice sites. Since the side planes of a free-standing wire should be free of strain and the presence of strain concentrators seems to be unlikely, the second model is favored.

The geometrical description of the twin formation is sketched in Fig. 6. During NW growth with the droplet in the quasi-stationary thermodynamic equilibrium a definite droplet wetting with contact angles dependent on the $\{1\,1\,2\}$-border plane polarity is adjusted (Fig. 6a). Disturbing the mechanical equilibrium of the droplet, i.e. due to convulsion or composition changes, in the way that the contact angles decrease, an inside directed mechanical line tension is created at the three-phase contact line (Fig. 6b). To compensate this line tension the system is driven to reduce the droplet–crystal contact area. At the $\{1\,1\,2\}_A$-border planes $\{1\,1\,1\}_A$-planes are formed (Fig. 6c). Due to geometrical reasons the $\{1\,1\,2\}_B$-border planes stay unchanged at this moment. After droplet relaxation the system seems to be unable to enlarge the droplet–crystal contact area by the formation of a suitable plane, i.e. (0 0 1). Thus, an outside directed line tension is produced. With further growth the contact area decreases and the line tension increases. If a sufficient line tension is reached, a rotational twin forms accompanied by the typical penetration angle and the formation of the corresponding $^{T}\{1\,1\,1\}_B$-planes at the $\{1\,1\,2\}_A$-border planes (Fig. 6d). Correspondingly, at the $\{1\,1\,2\}_B$-border planes the formation of $^{T}\{1\,1\,1\}_A$-planes becomes possible. The opposite $\{1\,1\,1\}$-planes proceed parallel and the contact area increases. This configuration seems to be unfavorable, because shortly after a further twin boundary is formed. Two different structures can be observed: (i) the twin

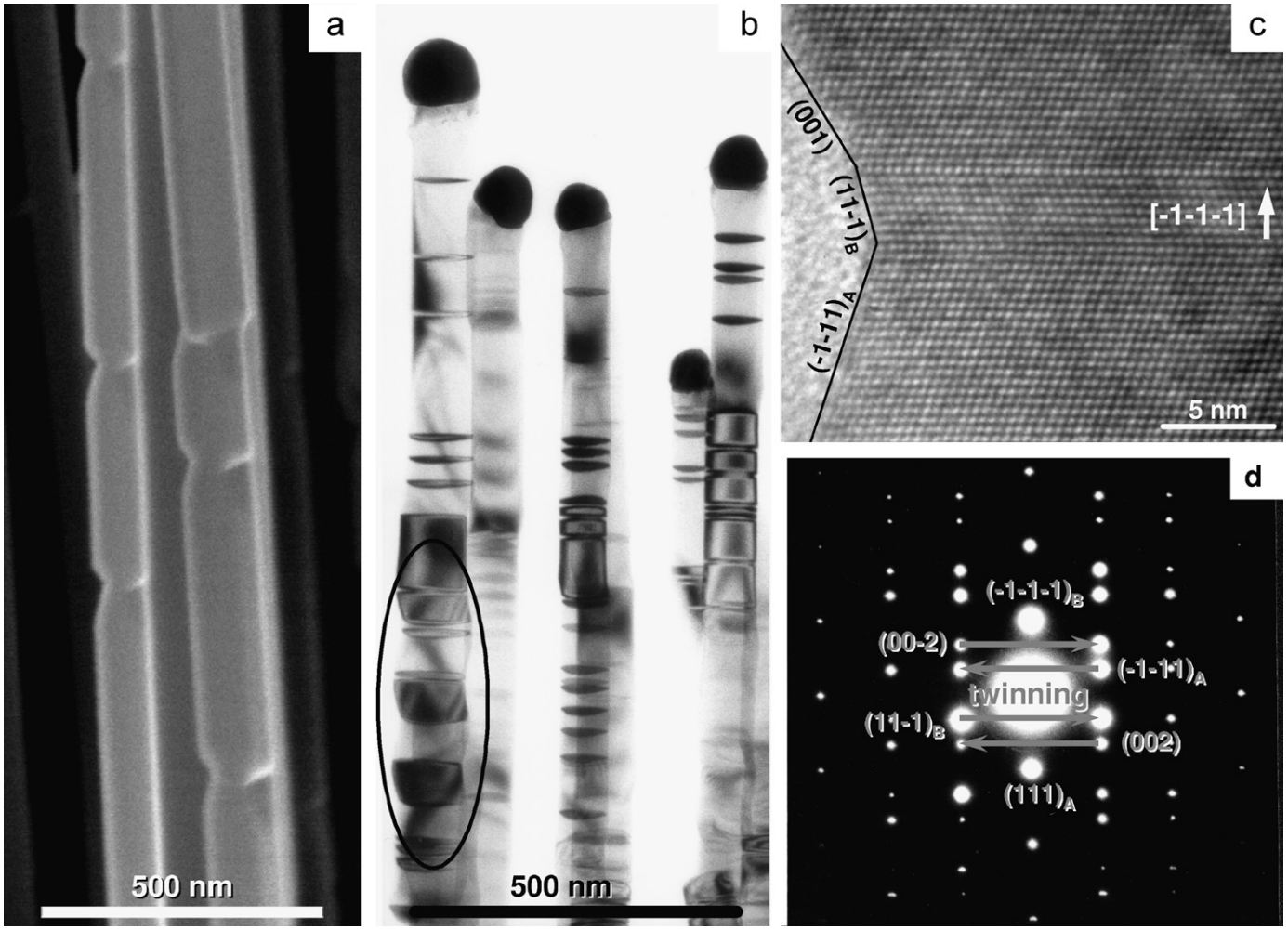

Fig. 5. The SEM image (a) ([1 $\bar{1}$ 0]-beam direction) and the bright-field TEM image (b) show the formation of lattice defects in $[\bar{1}\,\bar{1}\,\bar{1}]_B$-growth direction. These defects were identified in the HRTEM image (c) and the SAD pattern (d) (in both (1 $\bar{1}$ 0)-planes) as twin sections exclusively.

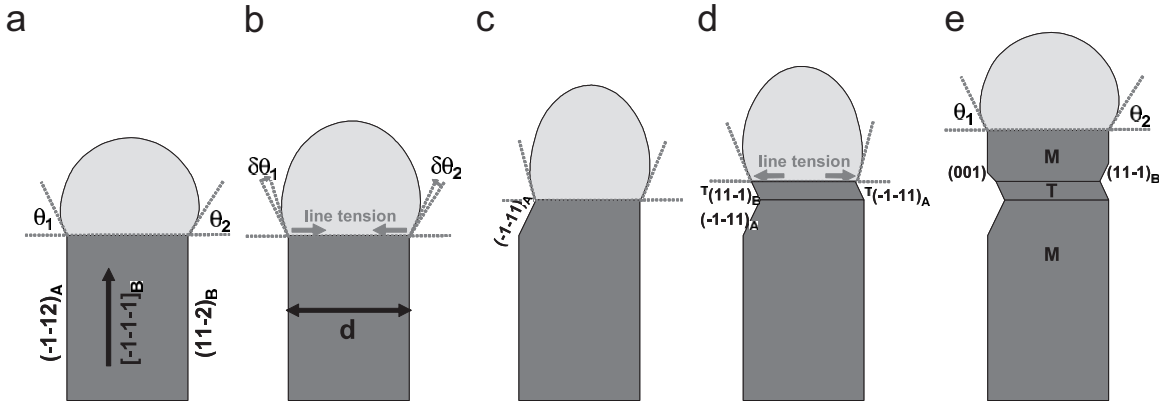

Fig. 6. Schematic illustration of the twin-formation mechanism.

switches in the matrix configuration with $\{1\,1\,1\}_A$-planes at the $\{1\,1\,2\}_A$-border planes and $\{1\,1\,1\}_B$-planes at the $\{1\,1\,2\}_B$-border planes. By continuing this twin boundary switching over several periods a zigzag morphology is formed (marked area in Fig. 5b). (ii) (Commonly observed case) the twin switches to $\{1\,0\,0\}$-planes at the $\{1\,1\,2\}_A$-border planes (Fig. 5c) and $\{1\,1\,1\}_B$-planes at the $\{1\,1\,2\}_B$-border planes. So, the contact area enlarges with growth. The effect of line tension is minimized by forming the original, stable $\{1\,1\,2\}$-border planes (Fig. 6e).

4. Conclusion

We studied the influence of the substrate preparation and the growth conditions important to fabricate GaAs NWs with metal-organic vapor phase epitaxy (MOVPE). Arranged GaAs-NW arrays could be achieved using nanosphere lithography. The growth parameters temperature, precursor partial pressures and growth duration were investigated. The growth rate limiting process depends strongly on the V/III ratio. The definite choice of the V/III ratio enables NW growth independent on the diameter. By investigating the temporal evolution of the GaAs-NW growth a diameter-dependent growth rate could be determined. For growth temperatures below 530 °C a column-shaped NW morphology is achieved. Otherwise, a tapered morphology is observed. Column-shaped GaAs NWs have {1 1 2}-border planes. The $\{1\,1\,2\}_B$-planes are more extended than the $\{1\,1\,2\}_B$-planes. During GaAs-NW growth rotational twins are incorporated. A crystallographic model is presented.

Acknowledgments

Dr. H. Herrnberger for the support in substrate preparation and gold evaporation. J. Lenzner for the help in SEM. F. Syrowatka and Dr. F. Heyroth for the ESEM images. The ''Deutsche Forschungsgemeinschaft'' for financial support.

References

[1] X. Duan, C. Lieber, Adv. Mater. 12 (4) (2000) 298.
[2] P. Yang, Y. Wu, R. Fan, Int. J. Nanosci. 1 (1) (2002) 1.
[3] J. Noborisaka, J. Motohisa, T. Fukui, Appl. Phys. Lett. 86 (2005) 213102.
[4] E. Givargizov, J. Crystal Growth 31 (1975) 20.
[5] V. Dubrovskii, N. Sibirev, G. Cirlin, Tech. Phys. Lett. 30 (8) (2004) 682.
[6] T. Tan, N. Li, U. Gösele, Appl. Phys. A 78 (2004) 519.
[7] R. Wagner, W. Ellis, Appl. Phys. Lett. 4 (1964) 89.
[8] K. Hiruma, M. Yazawa, K. Haraguchi, K. Ogawa, T. Katsuyama, M. Koguchi, H. Kakibayashi, J. Appl. Phys. 74 (5) (1993) 3162.
[9] K. Hiruma, M. Yazawa, T. Katsuyama, K. Ogawa, K. Haraguchi, M. Koguchi, H. Kakibayashi, J. Appl. Phys. 77 (2) (1995) 447.
[10] S. Bhunia, T. Kawamura, S. Fujikawa, Y. Watanabe, Physica E 24 (2004) 138.
[11] W. Seifert, et al., J. Crystal Growth 272 (2004) 211.
[12] T. Martensson, P. Carlberg, M. Borgström, L. Montelius, W. Seifert, L. Samuelson, Nano Lett. 4 (4) (2004) 699.
[13] E. Givargizov, Crystal Res. Technol. 10 (5) (1975) 473.
[14] J. Bauer, V. Gottschalch, B. Fuhrmann, in preparation.
[15] J. Bauer, V. Gottschalch, G. Wagner, in preparation.
[16] G. Stringfellow, Organometallic Vapor-Phase Epitaxy, second ed., Academic Press, San Diego, 1999, p. 47.
[17] U. Mareck, V. Gottschalch, E. Butter, Crystal Res. Technol. 24 (9) (1989) 887.
[18] P. Paufler, G. Wagner, Z. Krist. 191 (1990) 265.